Geomechanics and Engineering, *Vol. 37, No. 2 (2024) 189-195*
https://doi.org/10.12989/gae.2024.37.2.189

Beam models for continuous pipelines passing through liquefiable regions

Adil Yigit*

Istanbul Rumeli University, Civil Engineering Department, Istanbul, Turkiye

(*Received September 27, 2021, Revised March 5, 2024, Accepted April 6, 2024*)

Abstract. Buried pipelines can be classified as continuous and segmented pipelines. These infrastructures can be damaged either by ground movement or by seismic wave propagation during an earthquake. Permanent ground deformations (PGD) include surface faulting, liquefaction-induced lateral spreading and landslide. Liquefaction is a major problem for both superstructures and infrastructures. Buyukcekmece lake zone, which is the studied region in this paper, is a liquefaction prone area located near the North Anatolian Fault Line. It is an active fault line in Turkey and a major earthquake with a magnitude of around 7.5 is expected in this investigated region in Istanbul. It is planned to be constructed a new 12" steel natural gas pipeline from one side of the lake to the other side. In this study, this case has been examined in terms of two different support conditions. Firstly, it has been defined as a beam in liquefied soil and has built-in supports at both ends. In the other approach, this case has been modeled as a beam in liquefied soil and has vertical elastic pinned supports at both ends. These models have been examined and some solution proposals have been produced according to the obtained results. In this study, based on this sample, it is aimed to determine the behaviors of buried continuous pipelines subject to liquefaction effects in terms of buoyancy.

Keywords: buried continuous pipeline; earthquake; liquefaction; North Anatolian Fault Line; underground construction

1. Introduction

Liquefaction is one of the most important effects of an earthquake. It has a serious potential affecting both superstructures and infrastructures. Therefore, it has always been a focal point for some technical researches (Wu *et al.* 2018, Sonmezer 2019a,b, Gomez *et al.* 2019, Sonmezer *et al.* 2020, Kim *et al.* 2020, Ulker 2020, Isık *et al.* 2016, Ozocak *et al.* 2014). Any pipeline in liquefaction zone can be damaged by soil-pipe interaction and buoyancy effect during an earthquake (Nourzadeh *et al.* 2019). Some analysis have been carried out to investigate the underground structures- liquefiable soil interaction (Castiglia *et al.* 2018, Chou and Lin 2020, Sudevan *et al.* 2020). The other branch of this subject is submarine pipelines. These pipelines are usually buried in a shallow layer and this layer is usually composed of loose sand. This situation can cause to liquefaction, as well (Pisano *et al.* 2020). In literature, the pipeline-liquefaction interaction problem has been tried to be analyzed using model tests, finite element method and analytical approaches (Castiglia *et al.* 2021, Miyamoto *et al.* 2020, Valetti *et al.* 2018, Castiglia *et al.* 2020, Papadimitriu *et al.* 2019, Xia and Zhang 2018). In this study, two analytical models have been considered to investigate the effects of liquefaction on buried pipelines and the results of both cases have been examined. In addition, to mitigate the liquefaction effects on buried pipelines some approximations have been suggested.

*Corresponding author, Ph.D.
E-mail: adilyigit75@hotmail.com

Liquefaction occurs when saturated soil loses its shear strength. If there is a flat ground, such as the investigated region, and surrounding soil of pipeline quickly liquefies, the pipeline may uplift due to buoyancy. Hou and Liu (1990) have analyzed the pipeline strain caused by buoyancy effects, using the finite element method. In consequence of this analysis, the uplifting force per unit length has been described as follows

$$P_{uplift} = \frac{1}{4}\pi D^2(\gamma_{soil} - \gamma_{contents}) - \pi Dt\gamma_{pipe} \quad (1)$$

Where D and t are the diameter and thickness of the pipe, respectively; γ_{soil}, $\gamma_{contents}$ and γ_{pipe} are the unit weights of liquefied soil, pipe contents (oil, gas, water, etc.) and pipe material, respectively.

1.1 Regional seismicity

The North Anatolian Fault Line is a very active fault line in Turkey. Many significant earthquakes have occurred on this line throughout history as shown in figure (Fig. 1). 1939 Erzincan (M=7.9), 1942 Niksar-Erbaa (M=6.9), 1943 Tosya-Ladik (M=7.7), 1944 Bolu-Gerede (M=7.5), 1949 Karlıova (7.1), 1951 Kurşunlu (M=6.9), 1957 Abant (M=6.8), 1966 Varto (M=6.9), 1967 Mudurnu Valley (M=7.1), 1992 Erzincan (M=6.5), 1999 İzmit (M=7.4), 1999 Düzce (M=7.2) earthquakes are some examples of these historical records.

The North Anatolian Fault Zone (NAFZ) has two main branches in the Marmara Sea as the northern and the southern branches (Fig. 2). The northern branch of the NAFZ is very close to investigated liquefaction prone area. Many destructive earthquakes occurred in the Marmara Sea,

ISSN: 2005-307X (Print), 2092-6219 (Online)

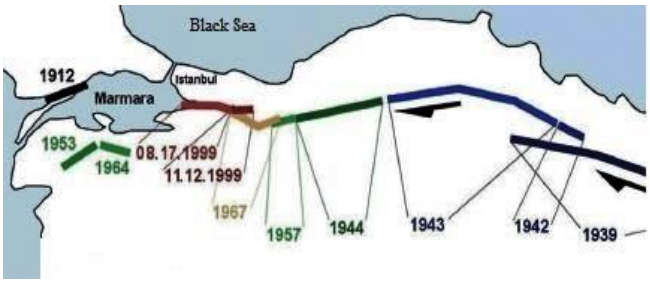

Fig. 1 Historical Earthquakes on The North Anatolian Fault Line (IBB 2019)

Fig. 2 The North Anatolian Fault Branches in the Marmara Sea (Yigit *et al.* 2018)

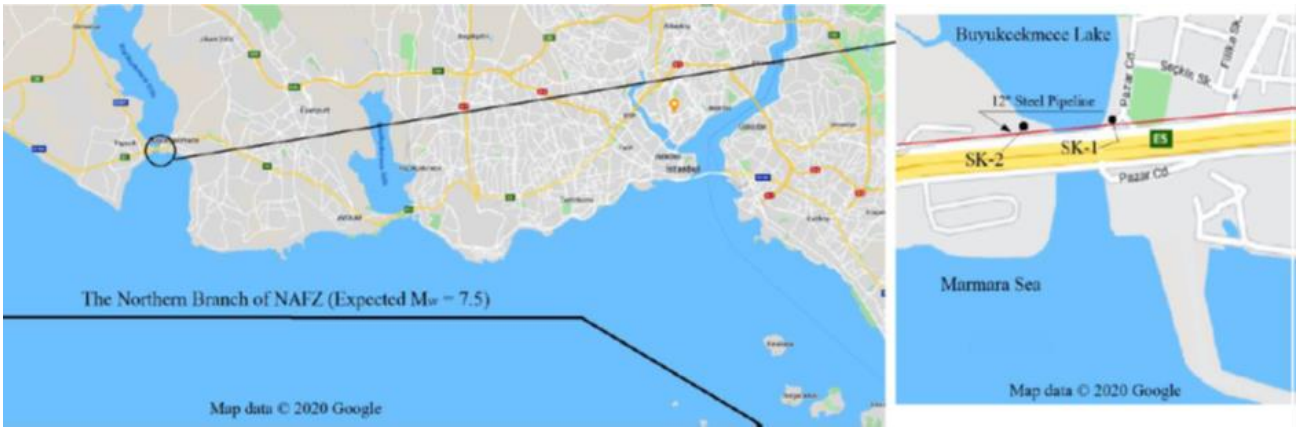

Fig. 3 The Northern Branch of NAFZ in The Marmara Sea (Map data © 2020 Google)

such as 1509 (M=7.6), 1719 (M=7.5), 1754 (M=7.5), 1766 (M=7.2 and M=7.6), 1894 (M=7.0), 1912 (M=7.4) and 1999 (M=7.4 and 7.1). Besides, a big earthquake with a magnitude between 7.0 and 7.5 is expected on the northern branch of NAFZ near the examined region (Fig. 3).

1.2 Regional geology

It is planned to combine the 12-inch steel natural gas pipelines available on both sides of Buyukcekmece Lake. The lake and its surrounding have weak ground. To investigate the ground of this area SK-1 and SK-2 boreholes were drilled (Fig. 3). It was observed that the groundwater level in both holes was 1.0 meter. The presence of loosely coupled fine sand containing fine gravel material was detected up to 20 meters deep. As a result of the investigations, it was determined that this region is sensitive to liquefaction under dynamic loads. Therefore, the expected earthquake increases the damage risk of the buoyancy effect for the hypothetical steel pipeline passed one side of the lake to the other side (Yigit 2007).

1.3 Failure criteria of continuous pipelines

Beside the values of strain allowed by manufacturers, for buried continuous pipelines under the effects of tension or compression, allowed strain criteria in table (Table 1) can be generally used, as well (IITK 2007). Where (in Table 1), ε_u is the failure strain of the pipe in tension; $\boldsymbol{\varepsilon_{cr-c}}$, $\boldsymbol{\varepsilon_{c-PGD}}$ and $\boldsymbol{\varepsilon_{c-wave}}$ have been described as below

Table 1 Allowable Strain Criteria for Buried Continuous Pipelines (IITK 2007)

Strain Component	Pipe Category	Allowable Strain	
		Tension	Compression
Continuous Oil and Gas Pipeline	Ductile Cast Iron Pipe	2%	For PGD: Onset of Wrinkling ($\boldsymbol{\varepsilon_{cr-c}}$)
	Steel Pipe	3%	
	Polyethylene Pipe	20%	For wave propagation:50% to 100% of the Onset of Wrinkling (0.5 to 1 $\boldsymbol{\varepsilon_{cr-c}}$)
	Bends and Tees of pipe	1%	
Continuous Water Pipeline	Steel and iron pipe	$0.25\varepsilon_u$ or 5%	$\boldsymbol{\varepsilon_{c-PGD}}$ $\boldsymbol{\varepsilon_{c-wave}}$

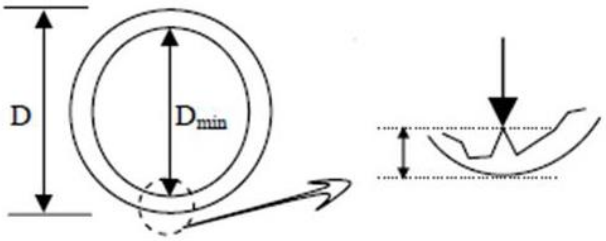

Fig. 4 Definition of D_{min} (IITK 2007)

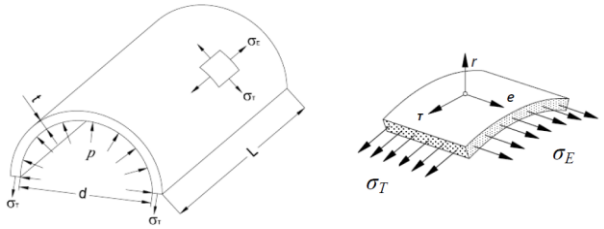

Fig. 5 Hoop and Longitudinal Stresses Due to Internal Pressure in a Pipe

$$\varepsilon_{cr-c} = 0.175\frac{t}{R} \tag{2}$$

$$\varepsilon_{cr-PGD} = 0.88\frac{t}{R} \tag{3}$$

$$\varepsilon_{cr-Wave} = 0.75\left[0.5\frac{t}{D'} - 0.0025 + 3000\left(\frac{PD}{2Et}\right)^2\right] \tag{4}$$

$$D' = \frac{D}{1 - \frac{3}{D}(D - D_{min})} \tag{5}$$

Where; t, R and D are the thickness, radius and diameter of the pipe, respectively. D_{min} has been described as in the figure (Fig. 4). P is the maximum internal operating pressure of the pipe and E is the modulus of elasticity.

1.4 Additional loads on pipelines

Operating pressure, soil (filler) weight, temperature change and traffic loads are significant additional effects on the buried pipelines. Comparing with the internal pressure (P_i=2.0 MPa), soil weight, temperature change and traffic loads have been neglected (Yigit 2018). In the case of thin-walled pipe under the effects of internal pressure, both hoop and longitudinal stress take place in the wall. In open-ended tube case (such as buried continuous pipelines) only hoop stress happens, longitudinal stress doesn't occur, as shown in Fig. 5. This hoop stress (σ_T) can be calculated as follows

$$\sigma_T = \frac{pD}{2t} \tag{6}$$

Where p, D, t are internal pressure, diameter of pipe and thickness of pipe wall, respectively. Strain caused by this stress should be taken into consideration when determining the ultimate allowable strain.

2. Modeling and solution of the problem

In this study, two main approximations have been taken into account. Primarily, the case of rigid pipe-ground connection at both edges of a liquefaction zone (to be referred as Case-I) has been studied (Fig. 6). Actually, in the investigated region, the surroundings of buried pipelines in the trench are filled with compacted sand during the construction of gas pipelines. Therefore, this case (to be referred as Case-II) may require the use of elastic supports instead of fixed supports, under the buoyancy forces (Fig. 7).

In both cases, it is assumed that the system and the pipe material within the elastic limits.

2.1 Examination of case-I

This approximation is valid when support points are fixed enough. To ensure this rigidity, special applications may be required at the support points. According to this, the case of liquefaction-pipeline interaction has been modeled as a beam under liquefaction load and has built-in supports at both ends as shown in Fig. 6. Depending on this approximation, the governing equation has been described as follows

$$EIv^{IV}(x) = q(x) \tag{7}$$

Where q(x) is a uniformly distributed load described as (Eq. (1))and to be referred as P_u. After the solution of this

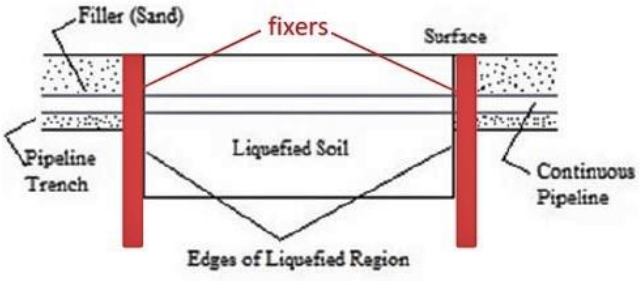

(a) Pipeline and Liquefied Zone for Case-I

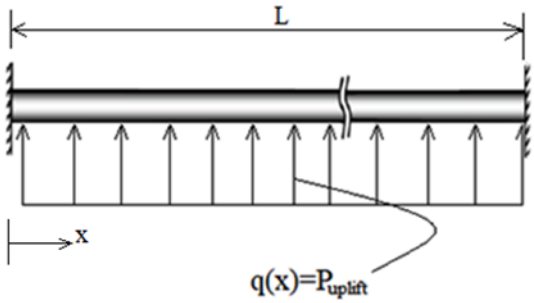

(b) Pipe-Soil Interaction Model for Case-I

Fig. 6 Case-I

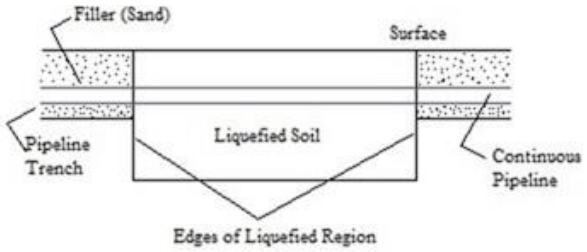

(a) Pipeline and Liquefied Zone Case-II

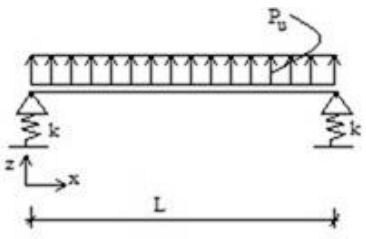

(b) Pipe-Soil Interaction Model for Case-II

Fig. 7 Case-II

governing equation, pipeline displacement (elastic curve) function for the investigated case can be obtained as below

$$v(x) = \frac{p_u L^4}{24EI}\left[\left(\frac{x}{L}\right)^2 - 2\left(\frac{x}{L}\right)^3 + \left(\frac{x}{L}\right)^4\right] \quad (8)$$

According to this well-known equation, the maximum strain ratio of cross-section of the pipe created by bending moment ($\varepsilon = \frac{M}{EI}y;\ y = \frac{D}{2}$) can be calculated from the following equation for the investigated case

$$\varepsilon_b = \frac{P_u D L^2}{24EI} \quad (9)$$

D is the diameter of the pipe and L is the width of the liquefied zone. The maximum axial strain, which occurs at maximum rotation point x=0.211L, can be obtained as follows

$$\varepsilon_a = -1 + \sqrt{1 + \left(\frac{P_u L^3}{125EI}\right)^2} \quad (10)$$

2.2 Examination of case-II

In this case, assuming that the connection between the filler material (sand) and the pipe is not strong enough as at the fixed support, the continuous pipeline on liquefied soil foundation has been defined as a beam which has hinged supports, which are elastic in the vertical direction, at both ends (Fig. 7). Using the governing equation (Eq. (7)), pipeline displacement (elastic curve) equation has been obtained as below

$$v(x) = \frac{p_u}{24EI}(x^4 - 2Lx^3 + L^3x) + z \quad (11)$$

Depending on this approximation, the maximum bending strain of cross-section of the pipe (ε_b) and the maximum axial strain (ε_a), which occurs at maximum rotation point x=0, have been obtained as (Eqs. (12) and (13)), respectively.

$$\varepsilon_b = \frac{P_u D L^2}{16EI} \quad (12)$$

$$\varepsilon_a = -1 + \sqrt{1 + \left(\frac{P_u L^3}{24EI}\right)^2} \quad (13)$$

Where; z is the maximum vertical displacement of elastic support. ASCE (1984) has defined the equivalent elastic soil spring coefficients as the ratio of maximum resistance divided by half of the maximum elastic deformation. According to this, in the case of upward direction vertical transverse movement, ASCE guideline suggests the following relations for sand

$$k_{wu} = \frac{2q_u}{z_u} \quad (14)$$

$$q_u = \bar{\gamma} H N_{qv} D \quad (15)$$

$$Z_u = (0{,}01 \sim 0{,}015)H \quad (16)$$

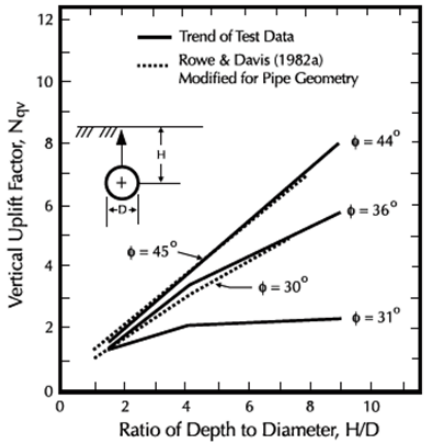

Fig. 8 N_{qv} for Sand (Trautmann and O'Rourke 1983)

k_{wu} and z_u to be referred as k and z, respectively. Coefficient of H can be used as 0.01 for this study (Yigit 2015). D is the pipe diameter, $\bar{\gamma}$ is the effective unit weight of the soil, H is the depth to center-line of the pipeline and N_{qv} is the vertical uplift factor for sand. N_{qv} is presented as a function of the depth over diameter ratio in Fig. 8.

3. Application to the studied area

3.1 Regional and material properties

The examined area is a liquefaction prone area. The length of the liquefied region, where the hypothetical natural gas pipeline will be placed, is 70 meters. The depth of the liquefaction zone is about 20 meters (Yigit 2007). The directional drilling method is one of the best ways to lay a pipeline under such that region. But the depth is very high and topography is not appropriate for this method. If the pipeline is planned to place through the liquefied zone, the effects of the liquefaction have to be thoroughly investigated. In this part, these effects have been examined.

In general, steel pipes (ST), covered by polyethylene, are used for natural gas transmission. The steel pipe in the investigated region has a 12 inch nominal diameter, 32.38 cm outer diameter and 0.556 cm thickness. The unit weight of the pipe material (steel) is $\gamma_{pipe} = 78.5\ kN/m^3$ and the unit weight of the natural gas is $\gamma_{contentz} = 0.0072\ kN/m^3$. Elasticity Modulus of steel is about $2x10^8$ kN/m^2.

The depth of the trench changes depending on the diameter of the pipe. The depth of the trench changes depending on the diameter of the pipe. The depth of the 12 inch steel pipe axis is H = 1.15 m, in the examined area. The surroundings of the buried pipe in the trench are filled with compressed sand. The unit weight of the filler sand is $\gamma = 15$ kN/m^3 and the angle of shear strength is $\varphi = 31^0$.

3.2 Solution of the approaches according to regional data

To determine the behaviors of buried continuous pipeline subject to liquefaction effects according to both approaches of this study, first of all, the uplifting force per unit length must be calculated. Depending on the materials properties, this force has been obtained from (Eq. (1)) as $P_u = 0.793\ kN/m$. For Case-I and Case-II, the maximum strains have been obtained as shown in Table 2.

Table 2 Obtained Strains for the Cases

Case-I		Case-II	
$\boldsymbol{\varepsilon_b}$	ε_a	ε_b	ε_a
0.0036	0.0119	0.0056	0.2838

Table 3 Ultimate Allowable Strains

Bending, $\boldsymbol{\varepsilon_{cr}}$	Tension, $\boldsymbol{\varepsilon_{aT}}$
0.00571	0.02972

The maximum bending and axial strain for the beam with fixed supports (Case-I) have been obtained as 0.0036 (from Eq. (9)) and 0.0119 (from Eq. (10)), respectively. For Case-II (the beam with vertical elastic pinned supports), the maximum bending strain has been obtained as 0.0056 (from Eq. (12)) and the maximum axial strain has been calculated as 0.2838 (from Eq. (13)).

4. Results

This problem should be examined in terms of the maximum strains and the maximum deflection of pipeline. In addition to not exceeding the material strength, the pipeline should not have a displacement in the upward direction more than the burial depth. Therefore, the maximum displacements of the models (Case-I and Case-II) are important for the safety of the pipelines. The allowable strain and displacement are upper limits for these approaches.

Local buckling is one of the most important limits for the strain ratio of pipe. The bending strain should be compared with this rate. Wrinkling limit has been described as (Eq. (2).) Depending on this equation, the local buckling limit has been calculated as 0.00601 for the studied pipe. Besides, for continuous oil and gas steel pipeline the allowable tensile strain is 3% as shown in Table 1. The axial strains should be compared with this limit. However, while making these comparisons, strain rates due to internal pressure mentioned as an operational strain should be deducted from these limits. Assuming that the pipe material is within the elastic limits, the operational strain due to the internal pressure has been obtained as 0.0003 from Equ.6. According to this, the ultimate allowable strains have been calculated as shown in Table 3 for the investigated pipeline.

Comparing Table 2 with Table 3, the bending and the axial strains are below the allowable values for Case-I. However, in Case-II, bending strain is very close to the limit and the strain due to tension exceeds too much the ultimate allowable axial strain, it is about ten times the allowable value. According to these outcomes, it can be concluded that the fixed support model is more appropriate than the pinned support model. Therefore, this suitable approximation should be applied.

Table 4 Theoretical Deflections of Beams

$\boldsymbol{\delta_I}$ (m)	$\boldsymbol{\delta_{II}}$ (m)	H_c (m)
3.5	17.6	1.0

Table 5 Critical Widths

Case-I, $\boldsymbol{L_{cr-I}}$ (m)	Case-II, $\boldsymbol{L_{cr-II}}$ (m)	L (m)
39	26	70

On the other hand, the pipeline maximum theoretical upward displacement must be less than the depth of the pipe. The hypothetical beam deflection has been calculated from (Eqs. (17) and (18)) for Case-I and Case-II, respectively (Table 4).

$$\delta_I = \frac{P_u L^4}{384EI} \tag{17}$$

$$\delta_{II} = \frac{5P_u L^4}{384EI} + Z_u \tag{18}$$

It is understood from these equations that δ_{II} approximately five times bigger than δ_I. Z_u calculated from Equ.16 as 0.01x1.15=0.0115 meter (H = 1.15). The depth from the top of the pipe to the ground surface (H_c) is about 1.0 meter for investigated case. Considering this value, it can be said that both deflections exceed too much (especially δ_{II}) the burial depth of the pipeline.

Taking as $\delta_{II}=H_c$, the maximum width of the liquefied zone can be predicted as (Eq. (19)) for Case-II. For Case-I, this value has been approximately estimated as L_(cr-I)=1.5L_(cr-II) . Critical depth H_{cr} can be calculated from Equ.20. Where; I_p is the importance factor and it can be taken as 2.6 according to IITK (2007). However, it should be suggested as I_p=3.0 for the liquefied region

$$L_{cr-II} = 3\left(\sqrt[4]{\frac{EIH_{cr}}{P_u}}\right) \tag{19}$$

$$H_{cr} = \frac{H_c}{I_p} \tag{20}$$

Under the conditions of the investigated region, L_{cr-II} and L_{cr-I} have been calculated as 26 meters and 39 meters, respectively. According to these values, the liquefied zone width (70 meters) is much more than the critical widths (Table 5).

Besides, according to the deflection of the beam, another main subject for Case-II is whether the elasto-plastic soil springs are under the limits or not. This issue should be checked depending on the shear force at the supports as the maximum shear force occurs at those vertical elastic points. Therefore, Z has been described as the displacement of this support under the uniformly distributed load (Eq. (21)).

$$Z = \frac{P_u L}{2k_{wu}} \tag{21}$$

Fig. 9 Example for Alternative Suggestion

Fig. 10 Implemented Project

This parameter has been calculated for the examined area as 0.0095 meter and it has been seen that Z=0.0095 < Z_u=0.0115. Depending on this comparison, it can be said that the model (Case-II) is within the elastic limits.

According to these results mentioned above, the application of Case-I is more convenient than the application of Case-II. However, both approximations have some failures and thus, it needs to be found another solution for the transition of the steel natural gas pipeline throughout the investigated liquefied prone area. Considering this situation, two projects have been designed that will bypass the effects of expected Big Istanbul Earthquake. The first suggestion has been designed as adjacent to the existing structure (bridge). Besides, as a separate structure, of which an example has been shown in Fig. 9, from the present bridge an alternative project has been recommended. Since the first proposal was less costly than the second proposal, it has been preferred and implemented as shown in Fig. 10.

5. Conclusions

It is important to avoid from seismically risky areas when designing buried pipelines in order not to be exposed to earthquake effects such as liquefaction. Directional drilling method is one of the best applications; if it can be implemented. When a buried pipeline is planned to be

placed in a zone with liquefaction risk, it should be conveniently restrained via additional applications at both sides of this zone so that the pipeline in liquefied area will be as a beam that has fixed supports at both ends. This static model gives more suitable results such as less strain and deflection. The great uplift displacement of submarine pipelines or the large deflection of pipelines in liquefied soil is not a desirable case. This failure situation should be controlled depending on the burial depth of pipe and/or critical length of pipe in liquefied zone. On the other hand, bypassing any risky area such as liquefied region via a structure such as bridge is one of the most certain solutions for pipelines.

This paper submits a good solution when the problem remains within the elastic limit. However, beyond the elastic limit cases can be examined in the future studies.

References

American Society of Civil Engineers (ASCE) (1984), Guidelines for the Seismic Design of Oil and Gas Pipeline Systems, Committee on Gas and Liquid Fuel Lifeline, ASCE.

Castiglia, M., Magistris, F.S., Onori, F. and Koseki, J. (2021), "Response of buried pipelines to repeated shaking in liquefiable soils through model tests", *Soil Dyn. Earthq. Eng*., 143. https://doi.org/10.1016/j.soildyn.2021.106629.

Castiglia, M., Fierro, T. and Magistris, F.S. (2020), "Pipeline performances under earthquake-induced soil liquefaction: State of the art on real observations, model tests, and numerical simulations", *Shock Vib*., 2020. https://doi.org/10.1155/2020/8874200.

Castiglia, M., De Magistris, F.S. and Napolitano, A. (2018), "Stability of onshore pipelines in liquefied soils: Overview of computational methods", *Geomech. Eng*., **14**(4), 355-366. https://doi.org/10.12989/gae.2018.14.4.355.

Chou, J. and Lin, D. (2020), "Incorporating ground motion effects into Sasaki and Tamura prediction equations of liquefaction-induced uplift of underground structures", *Geomech. Eng*., **22**(1), 25-33. https://doi.org/10.12989/gae.2020.22.1.025.

Hou, Z., Cai, J. and Liu, X. (1990), "Response calculation of oil pipeline subjected to permanent ground movement induced by soil liquefaction", *Proceedings of the China-Japan Symposium on Lifeline Earthquake Engineering*, Beijing, China.

Indian Institute of Technology (IITK, 2007), Guidelines for Seismic Design of Buried Pipelines. İndian: Kanpur.

Isık, A., Unsal, N., Gurbuz, A. and Sisman, E. (2016), "Assessment of liquefaction potential of Fethiye based on spt and shear wave velocity", *J. Fac. Eng. Architect. Gazi Univ*., **31**(4), 1027-1037. https://doi.org/10.17341/gummfd.12917.

Istanbul Büyükşehir Belediyesi (IBB), Deprem ve Zemin İnceleme Müdürlüğü (2019), İstanbul Deprem Çalıştayı, İstanbul, Turkiye (In Turkish).

Kim, H., Kim, M., Baise, L.G. and Kim, B. (2020), "Local and regional evaluation of liquefaction potential index and liquefaction severity number for liquefaction-induced sand boils in pohang, South Korea", *Soil Dynam. Earthq. Eng*., **141**(9). https://doi.org/10.1016/j.soildyn.2020.106459

Miyamoto, J., Sassa, S., Tsurugasaki, K. and Sumida, H. (2020), "Wave-Induced liquefaction and floatation of a pipeline in a drum centrifuge", *J. Waterw. Port Coast. Ocean Eng*., **146**(2). https://doi.org/10.1061/(ASCE)WW.1943-5460.0000547.

Molina-Gomez, F., Caicedo, B. and Viana da Fonseca, A. (2019), "Physical modelling of soil liquefaction in a novel micro shaking table", *Geomech. Eng*., **19**(3), 229-240. https://doi.org/10.12989/gae.2019.19.3.229.

Nourzadeh, D., Mortazavi, P., Ghalandarzadeh, A., Takada, S. and Ahmadi, M., (2019), "Performance assessment of the Greater Tehran Area buried gas distribution pipeline network under liquefaction", *Soil Dynam. Earthq. Eng*., **124**, 16-34. https://doi.org/10.1016/j.soildyn.2019.05.033.

Ozocak, A. and Tapan, M. (2014), "The influence of pore size distribution and radial consolidation properties on the liquefaction potential of silts", *J. Fac. Eng. Architect.Gazi Univ*., **29**(1), 35-47.

Papadimitriou, A.G., Bouckovalas, G.D., Nyman, D.J. and Valsamis, A.I. (2019), "Analysis of buried steel pipelines at watercourse crossings under liquefaction-induced lateral spreading", *Soil Dyn. Earthq. Eng*., **126**. https://doi.org/10.1016/j.soildyn.2019.105772.

Pisanò, F., Cremonesi, M., Cecinato, F. and Vecchia, G.D. (2020), "CFD-Based framework for analysis of soil-pipeline interaction in reconsolidating liquefied sand", *J. Eng. Mech*., **146**(10). https://doi.org/10.1061/(ASCE)EM.1943-7889.0001846.

Sonmezer, Y.B., Akyuz, A. and Kayabali, K. (2020), "Investigation of the effect of grain size on liquefaction potential of sands", *Geomech. Eng*., **20**(3), 243-254. https://doi.org/10.12989/gae.2020.20.3.243.

Sonmezer, B.Y. (2019a), "Energy-based evaluation of liquefaction potential of uniform sands", *Geomech. Eng*., **17**(2), 145-156. https://doi.org/10.12989/gae.2019.17.2.145.

Sonmezer, B.Y. (2019b), "Investigation of the liquefaction potential of fiber-reinforced sand", *Geomech. Eng*., **18**(5), 503-513. https://doi.org/10.12989/gae.2019.18.5.503.

Sudevan, P.B., Boominathan, A. and Banerjee, S., (2020), "Mitigation of liquefaction-induced uplift of underground structures by soil replacement methods", *Geomech. Eng*., **23**(4), 365-379. https://doi.org/10.12989/gae.2020.23.4.365.

Trautmann, C.H. and O'Rourke, T.D. (1983), "Load-displacement characteristics of a buried pipe affected by permanent earthquake ground movements", Earthquake Behavior and Safety of Oil and Gas Storage Facilities, Buried Pipelines and Equipment, PVP-77, ASME, New York, June, 254-262.

Ulker, M. (2020), "Comparative study of numerical formulations developed for constitutive modeling of static and dynamic behavior of saturated sands: Proposal of a new hardening law", *J. Fac. Eng. Architect. Gazi Univ*., **35**(3), 1353-1368. https://doi.org/10.17341/gazimmfd.528145.

Valleti, D., Sivaranjani, S., Shahin, C. and Mondal, S. (2018), "Design of buried flexible pipelines during liquefaction", *Int. J. Eng. Technol*., **7**(2). https://doi.org/10.14419/iijet.v7i2.21.12263.

Wu, Y., Hyodo, M. and Aramaki, N. (2018), "Undrained cyclic shear characteristics and crushing behaviour of silica sand", *Geomech. Eng*., **14**(1), 1-8. https://doi.org/10.12989/gae.2018.14.1.001.

Xia, M. and Zhang, H. (2018), "Stress and deformation analysis of buried gas pipelines subjected to buoyancy in liquefaction zones", *Energies*, **11**(9), 2334. https://doi.org/10.3390/en11092334.

Yiğit, A., Lav, M.A. and Gedikli, A. (2018), "Vulnerability of natural gas pipelines under earthquake effects", *J. Pipeline Syst. Eng. Pract.*, **9**(1). https://doi.org/10.1061/(ASCE)PS.1949-1204.0000295

Yigit, A. (2015), "Buried continuous pipelines under the effects of earthquake", PhD Thesis, Istanbul Technical University, September, Istanbul, Turkey.

Yigit, A. (2007), Gomulu Boru Hatlarının Deprem Etkilerine karsı Davranısı, Yuksek Lisans Tezi, I.T.U. Fen Bilimleri Enstitusu, Mayıs. (In Turkish).

CC